Detection of Radio Frequency Interference with the Aquarius Radiometer

Christopher Ruf and Sidharth Misra
Space Physics Research Laboratory, University of Michigan
2455 Hayward St., Ann Arbor, MI, 48109-2143 USA
734-764-6561 (V), 734-936-0503 (F), cruf@umich.edu (E)

***Abstract* — An algorithm is developed to detect the presence of Radio Frequency Interference (RFI) with the Aquarius Radiometer. The detection algorithm identifies individual samples of the antenna temperature that deviate significantly from the average value of nearby samples. The algorithm is tested and characterized using a new form of RFI "ground truth" that is based on measurements of the kurtosis of the amplitude distribution of the pre-detected signal. With ground truth available, adjustable parameters of the algorithm can be optimized.**

Keywords - microwave radiometry, radio frequency interferences, kurtosis, Aquarius

I. BACKGROUND

The Aquarius mission includes an L-Band microwave radiometer in low earth orbit to measure sea surface salinity (SSS) [2]. The mission is intended to produce global maps of SSS for use in climate studies. Contamination of these data records is possible if manmade sources or Radio Frequency Interference (RFI) are mistakenly detected and interpreted as natural radio emission by the ocean surface. The presence of RFI has been noted in a number of spaceborne microwave radiometers at higher frequencies than Aquarius [4] and on airborne radiometers operating at the same frequency as Aquarius [1]. The sensitivity of the observed L-Band brightness temperature to climatically relevant changes in SSS is low enough that even quite small biases in the observations, due to Radio Frequency Interference (RFI), can be detrimental to the mission objectives [8]. For this reason, the radiometer's data sampling rate has been increased by several orders of magnitude above the Nyquist rate suggested by the antenna footprint size and the spacecraft orbital velocity. This will significantly enhance the flexibility and sensitivity of an RFI "glitch detection" algorithm that will be included as part of the ground processing.

The Aquarius RFI detection algorithm operates on samples of the brightness temperature at their raw (highest) sample rate. It is designed to detect individual samples that differ significantly from the local average value of those nearest neighbor samples that are themselves not corrupted by RFI. There are a number of parameters in the detection algorithm which can be adjusted to control its behavior. Those parameters affect: a) the extent of the region surrounding a sample which constitutes its local neighborhood; b) the magnitude of the difference between a sample and its local average which indicates the presence of RFI; and c) the "guard band" surrounding a sample with RFI that will also be flagged as potentially contaminated. In addition, optimal values for the parameters may vary depending on the proximity of a sample to a major coastline. The behavior of the detection algorithm can be characterized in several ways. The probability of false alarm characterizes excessive sensitivity, in which case RFI is indicated when it is not present. This possibility is more likely near a major coastline, when the natural variations in brightness temperature are greatest, than it is in the open ocean. The probability of missed detection characterizes inadequate sensitivity of the algorithm to the presence of RFI. The settings of the parameters in the algorithm must weigh these two competing characteristics against one another in order to reach an acceptable compromise.

A series of field campaigns have recently been conducted with a new type of microwave radiometer that uses an Agile Digital Detector (ADD) to measure both the 2^{nd} and 4^{th} moments of the pre-detection voltage [3, 5, 6]. The 2^{nd} moment is the conventional measurement made by a square-law detector. The additional 4^{th} moment measurement allows the kurtosis of the voltage to be calculated. The kurtosis has been found to be a very reliable indicator of the presence of RFI, even when its power level is extremely low. Data from the ADD field campaigns, if taken at the proper sample rate, can be used as an experimental test bed for assessing the behavior of the Aquarius RFI detection algorithm as functions of its adjustable parameters. In particular, the availability of the kurtosis measurements allows for the determination of the probability of missed detection of the algorithm, a statistic that is otherwise difficult to estimate accurately.

An overview of the Aquarius RFI detection algorithm is described, followed by a characterization of its performance using ADD field campaign data.

II. DESCRIPTION OF RFI DETECTION ALGORITHM

The RFI detection algorithm can be broken into five steps:

1) Identify the set of TA samples surrounding the sample under test which will be used to estimate the local mean value of TA. The interval of time that those samples must lie within is constant in order to keep constant the ground track distance covered by the antenna footprint. However, because the spacing between samples of TA is not uniform, the actual

Sponsored by NASA/ESTO NNG05GL97G

number of samples that fall in the time interval will vary. (Relevant parameter of algorithm – Ws)

2) The TA samples surrounding the sample under test are examined for the presence of RFI. They are considered to be contaminated by RFI if they deviate from the local mean by more than a specified threshold. The threshold is specified as a multiple of the NEΔT radiometric uncertainty of a single sample of the antenna temperature. The samples are also checked for being flagged as RFI from previous tests. (Relevant parameter of algorithm – Tm)

3) Samples that pass the test are averaged together to estimate the local "clean" mean value of the sample under test. The average should equally weight samples made before and after the sample under test, in order to best represent the gradient of TA along the ground track of the radiometer.

4) The TANT sample under test is compared to the local "clean" mean. It is considered to be contaminated by RFI if it deviates from the local mean by more than a specified threshold. The threshold is specified as a multiple of the NEΔT radiometric uncertainty of a single sample of the antenna temperature. This test may be less strict than the one in step 2 because occasional false alarms will not have much of an effect on the determination of the local mean but they will directly result in lost data at this stage. (Relevant parameter of algorithm – Tdet)

5) If TANT is determined to be contaminated by RFI, a specified range of samples surrounding it is also flagged as contaminated. This range will be determined based on the characteristic time scale with which signals can enter and leave the radiometer antenna beam vs. the time interval between raw samples. Some samples made while the Correlated Noise Diode (CND) is ON may (and generally will) also fall within the specified range. Because the CND is coupled into the signal with a TA background, these samples may also be contaminated by RFI and should be flagged as such. (Relevant parameter of algorithm – W)

For all results presented below, the adjustable parameters of the RFI detection algorithm have the following values: Ws=20; Tm=1.5,; Tdet=4,; W=5.

III. RFI Detection Algorithm Perfromance

A ground based campaign was conducted during April-May 2006 at JPL with the JPL-PALS RF front end [7] and University of Michigan Agile Digital Detector back end [5]. The sampling characteristics of the measurements and the controlled variation of the observed TB scene were similar enough to the expected conditions with Aquarius on orbit so that these measurements can be used to assess the expected performance of the Aquarius RFI detection algorithm.

ADD measures the 1st – 4th moments of the amplitude distribution of the pre-detected signal. The 2nd moment is a traditional square law detector. The kurtosis is derived from 2nd and 4th central moments. It provides a reliably means to identify the presence of RFI with power levels at or above the radiometer NEΔT [5].

Relevant characteristics of the Aquarius on-orbit data sampling are:

- Calibrated TB samples are measured every 10ms
- Satellite ground track velocity is ~ 7.5km/s
- Radiometer HPBW footprint diameters are ~ 85, 102 and 125 km

As a result of these characteristics, a very sharp TB feature, such as a coastal crossing, requires approximately 13 seconds (= HPBW/$v_{groundtrack}$) to develop in the Aquarius image. In addition, there will be approximately 1300 TB samples taken during a coastal crossing transition as the complete antenna footprint passes over the coastline. This can be expected to be one of, if not the, most rapid naturally occurring TB transition while on orbit. One concern is that possible RFI false alarms will occur during these rapid changes in TB.

To address the performance of the proposed Aquarius RFI detection algorithm, PALS-ADD data have been analyzed as a proxy for Aquarius flight data. The data sample rate is similar to that of Aquarius so that the performance of the RFI algorithm with PALS-ADD will be roughly indicative of that with Aquarius. One example is shown in Fig. 1 while viewing the nadir sky. The top panel in the figure is a 60 s time series of the 2nd moment of the pre-detection signal. The 2nd moment is proportional to the system noise temperature of the radiometer and includes the effects of the downwelling sky brightness, of thermal emission by the radiometer's antenna and the cabling between the antenna and receiver, and of the noise temperature of the receiver itself. The 2nd moment measured by ADD is equivalent to the standard "antenna counts" that are measured as Level 0 data products of conventional radiometers that use analog detectors. The sharp spikes in the top panel are caused by RFI, which was ubiquitous during daytime weekday operation at JPL. The center panel if Fig.1 shows the result of an RFI detection algorithm based on measurements of the kurtosis. A vertical bar is present whenever the kurtosis deviates from its nominal value by more than 3.7 times the standard error in the estimate of the kurtosis (estimated using the number of independent samples available during a single integration time). The bottom panel shows the results of the proposed Aquarius RFI detection algorithm, acting on the time series of the 2nd moment. The large RFI spikes that are visible in the top panel are easily detected by the algorithm. RFI events with a lower 2nd moment are detected by the kurtosis algorithm but not the 2nd moment algorithm. The kurtosis can thus be used as a form of RFI "ground truth" to evaluate the performance of the 2nd moment algorithm.

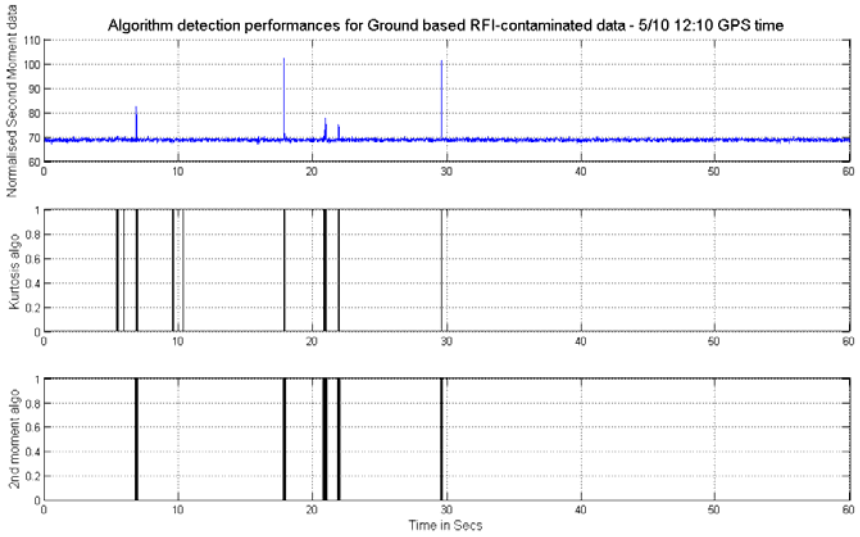

Figure 1. RFI detection of PALS-ADD L-Band radiometer measurements of nadir sky view with strong RFI present: (top) 2nd moment time series; (center) kurtosis of signal shows all RFI present; (bottom) Aquarius RFI detection algorithm catches most but not all RFI.

A second example is shown if Fig.2. In this case, a blackbody absorber was slowly passed in front of the PALS antenna while it was viewing the nadir sky. There was no noticeable RFI present at this time. The rate at which the absorber was moved into the antenna beam approximately matches the rate at which a coastline would enter the Aquarius antenna footprint on orbit. The top panel again shows the 2nd moment samples. The simulated coastal crossing occurs at approximately 45 seconds elapsed time. The center panel shows that the kurtosis-based RFI detection algorithm detects no RFI. The bottom panel shows the 2nd moment–based RFI detection algorithm. Here, a number of RFI false alarm instances. In particular, note that the probability of a false alarm is greater in the vicinity of the rapid changes in TB that are present during the coastal crossing. This suggests that the Aquarius detection threshold may need to be varied as a function of the location of the footprint – to be less susceptible to rapid dTB/dt variations near coastlines.

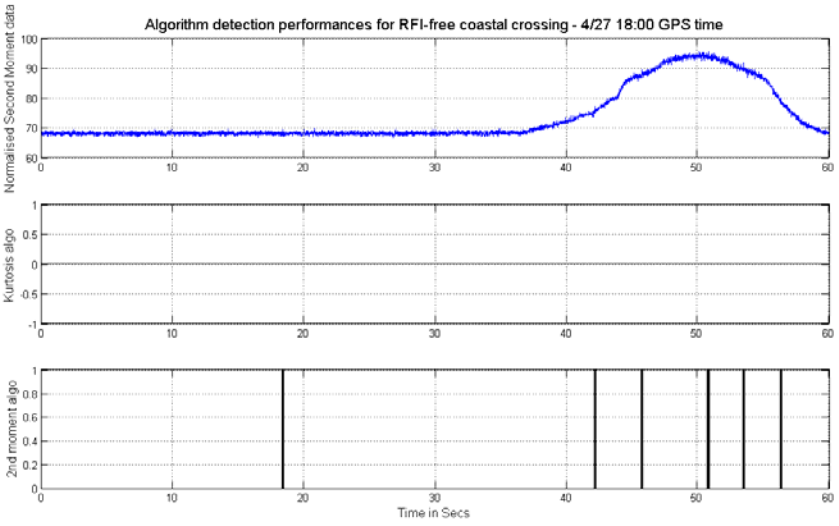

Figure 2. PALS-ADD L-Band radiometer measurements during transition from nadir sky view to BB absorber. Rate of change of TB during transition matches that of Aquarius radiometer during coastal crossing. (top) 2nd moment time series; (center) kurtosis of signal shows no RFI present; (bottom) Aquarius RFI detection algorithm has some false alarm – they are more likely when the TB is changing quickest.

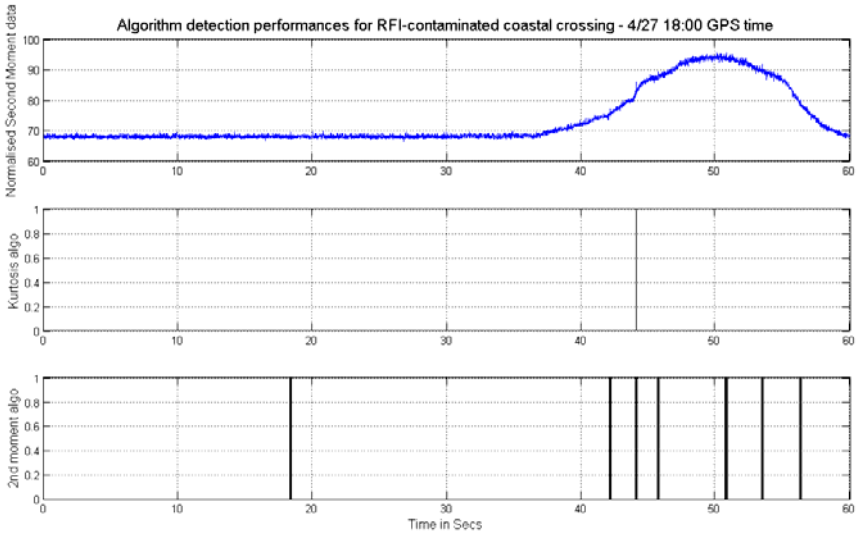

Figure 3. Similar to Fig. 2 but with a single RFI event artificially added at the point of maximum time-rate-of-change of TB during simulated coastal crossing. (top) 2nd moment time series; (center) kurtosis of signal detects single RFI event; (bottom) Aquarius RFI detection algorithm detects the true RFI event as well as the false alarms.

A third example is shown in Fig. 3. In this case, the time series from Fig. 2 is artificially modified by adding a single RFI event at approximately 44 seconds elapsed time. This is intended to represent, for example, an air traffic control radar located on the coast. The kurtosis detector (center panel) identifies the single RFI event. The 2nd moment algorithm also successfully identifies it, along with the other false alarm detections that were previously noted. This verifies that the 2nd moment algorithm is capable of detecting coastal RFI when the background TB is changing rapidly.

IV. SUMMARY

A "glitch detection" algorithm is proposed for the Aquarius radiometer to identify the presence of RFI. Algorithm performance has been demonstrated by examples with adjustable parameters of the algorithm set as follows:

Averaging window for local mean TB value: Ws=20
Mean threshold to select clean TBs for local mean: Tm=1.5
Detection threshold to decide if RFI is present: Tdet=4
Neighborhood of detected RFI also flagged: W=5

The performance of the algorithm has been characterized using a new form of RFI "ground truth" that is based on measurements of the kurtosis of the amplitude distribution of the pre-detected radiometer signal. Kurtosis-based RFI detection can reliably identify the presence of RFI that is at or near the NEΔT radiometric noise floor. The performance of the Aquarius RFI detection algorithm has been examined using several case study examples. It is found that there is an enhanced susceptibility to erroneous detection of RFI (i.e. false alarms) when the brightness temperature of the scene under observation is changing rapidly, such as when passing over a coastline. An experiment that simulates the expected time-rate-of-change of the observed brightness temperature during a costal crossing has been conducted and it is found that the detection threshold can be adjusted to control the probability of false alarms, via the adjustable parameter Tdet. This parameter sets the threshold deviation from the local mean at which the RFI flag is triggered. For the Aquarius flight algorithm, it is anticipated that Tdet will be adjusted dynamically as a function of the latitude and longitude of the antenna footprint.

REFERENCES

[1] Le Vine, D.M., "ESTAR Experience with RFI at L- band and Implications for Future Passive Microwave Remote Sensing from Space," Proc. IGARSS 2002, Toronto, Canada.

[2] Le Vine, D.M., G.S.E. Lagerloef, F. Pellerano, S. Yueh, and R. Colomb, 2006: Aquarius: A Mission to Monitor Sea Surface Salinity from Space, Proc. 2006 IEEE International Geoscience and Remote Sensing Symposium, Denver, CO, 31 Jul - 4 Aug 2006.

[3] Misra, S., C.S. Ruf and R. DeRoo, "Agile Digital Detector for RFI Mitigation," 2006 Specialist Meeting on Microwave Radiometry, San Juan, PR, 28 Feb – 3 Mar 2006.

[4] Njoku, E. G., P. Ashcroft, T. K. Chan, and L. Li,``Global survey and statistics of radio-frequency interference in AMSR-E land observations," *IEEE Trans. Geosc. Rem. Sens*., vol. 43, pp. 938--947, 2005.

[5] Ruf, C.S., S. M. Gross and S. Misra, "RFI Detection and Mitigation for Microwave Radiometry with an Agile Digital Detector," IEEE Trans. Geosci. Remote Sens.,44(3), 694-706, 2006.

[6] Ruf, C., S. Misra, S. Gross and R. De Roo, "Detection of RFI by its Amplitude Probability Distribution," Proc. 2006 IGARSS, Denver, CO, 31 Jul - 4 Aug 2006.

[7] Wilson, William J., Simon H. Yueh, Steven J. Dinardo, Seth Chazanoff, Fuk Li, and Y. Rahmat-Samii, "Passive Active L- and S-band (PALS) Microwave Sensor for Ocean Salinity and Soil Moisture Measurements," IEEE Trans. Geosci. Remote Sensing, 39, 1039-1048, 2001.

[8] Yueh, S.H., R. West, W.J. Wilson, F.K. Li, E.G.Njoku and Y. Rahmat Samii, "Error sources and feasibility for microwave remote sensing of ocean surface salinity, *IEEE Trans. Geosci. Remote Sens*., 39, 2001.